Missouri University of Science and Technology
Scholars' Mine

International Conferences on Recent Advances in Geotechnical Earthquake Engineering and Soil Dynamics

1991 - Second International Conference on Recent Advances in Geotechnical Earthquake Engineering & Soil Dynamics

14 Mar 1991, 10:30 am - 12:30 pm

Applicability of Effective Stress Analysis for the Soil-Structure System in Design Practice

Shunji Fujii
Taisei Corporation, Tokyo, Japan

Follow this and additional works at: https://scholarsmine.mst.edu/icrageesd

Part of the Geotechnical Engineering Commons

Recommended Citation

Fujii, Shunji, "Applicability of Effective Stress Analysis for the Soil-Structure System in Design Practice" (1991). *International Conferences on Recent Advances in Geotechnical Earthquake Engineering and Soil Dynamics*. 7.
https://scholarsmine.mst.edu/icrageesd/02icrageesd/session03/7

This work is licensed under a Creative Commons Attribution-Noncommercial-No Derivative Works 4.0 License.

This Article - Conference proceedings is brought to you for free and open access by Scholars' Mine. It has been accepted for inclusion in International Conferences on Recent Advances in Geotechnical Earthquake Engineering and Soil Dynamics by an authorized administrator of Scholars' Mine. This work is protected by U. S. Copyright Law. Unauthorized use including reproduction for redistribution requires the permission of the copyright holder. For more information, please contact scholarsmine@mst.edu.

Proceedings: Second International Conference on Recent Advances in Geotechnical Earthquake Engineering and Soil Dynamics, March 11-15, 1991, St. Louis, Missouri, Paper No. 3.10

Applicability of Effective Stress Analysis for the Soil-Structure System in Design Practice

Shunji Fujii
Principal Engineer, Taisei Corporation, Tokyo, Japan

SYNOPSIS : In the design process of a high rise building in Niigata City, the prediction of liquefaction potential has been conducted by comparing liquefaction resistance obtained from laboratory tests , with shear stress obtained in a total stress analysis of a soil-structure model. As an attempt, one dimensional and two dimensional effective stress analysis were carried out by using a computer program DIANA . By the comparison of these analytical results, the applicability of the effective stress analysis to the actual soil-structure system has been examined.

INTRODUCTION

The author is involved in the design of a high rise building in Niigata City, Japan, where significant damages from liquefaction were observed in the 1964 earthquake. For the design of this building an examination of the liquefaction potential was considered essential. For the prediction of liquefaction potential of sand, the methods are roughly classified into the following three categories:

1) Examination of the soil profile.

2) Comparison of cyclic strength against liquefaction obtained by laboratory test, with expected shear stress during earthquakes.

3) Effective stress analysis

For the design practice, a dynamic analysis of soil-structure model was carried out by using the total stress method. The nonlinearity of the soil was approximated by an equivalent linear method. The prediction of the liquefaction potential was conducted by comparing the numerically obtained effective shear stress with the cyclic strength against liquefaction obtained from a laboratory test.

Though several different computer programs and constitutive models of sand for the effective stress analysis have been proposed , researchers are still trying to verify the numerical procedure, by comparing the numerical results with shaking table tests or centrifugal tests. There have not been many applications of the effective stress analysis to the prediction of liquefaction in a design practice. Therefore in this study, the author has carried out an effective stress analysis of the actual soil deposit and soil-structure system, and by comparing the results with the total stress analysis, the applicability of the effective stress analysis for the design purpose have been attempted.

SITE CONDITION AND BUILDING

The site, which is located in the city of Niigata, Japan, is about 1 km from the Shinano river, and this area suffered minor damages in the 1964 earthquake. The planned building as described in Fig. 1 has 20 stories above ground and 3 stories under ground, which is supported on a pile foundation reaching a stiff sand at GL-40m. The pile foundation was mainly selected to maintain the structural safety ,specifically in the case of liquefaction under the basemat.

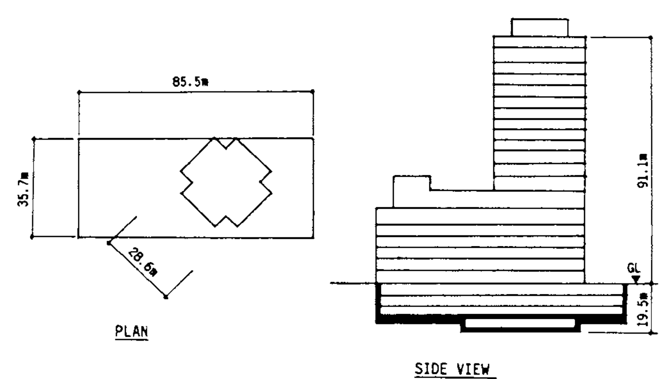

Figure 1 Description of Building

Figure 2 shows the soil profile and the distribution of N-value. The surface soil is sand to the depth of -65m, and with silty soil between -65 m to -100 m, the bed rock lies 144 m below the ground surface. The N- value gradually increase as the depth increases to the depth of -25 m and is relatively constant in the sand layer below . Though the soil property is better in this area than those areas where severe damage from liquefaction was observed during 1964 earthquake, having the water level as shallow as -1.5 m, liquefaction of the surface soil is expected from the design earthquake and the estimation of the liquefaction potential needs to be carried out.

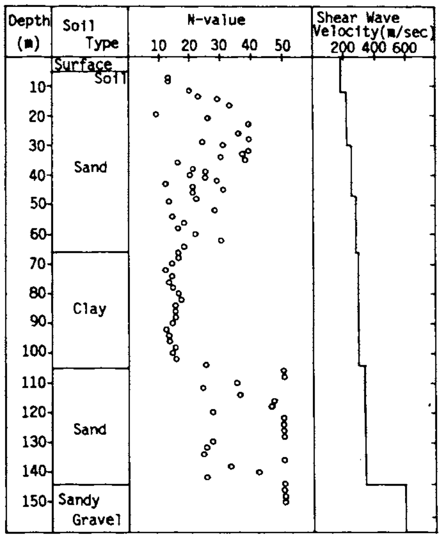

Figure 2 Soil Profile and N - value

PREDICTION OF LIQUEFACTION POTENTIAL

Prediction of the liquefaction potential in the design was conducted by comparing the cyclic strength of the soil against liquefaction and the shear stress level expected in the design earthquake.

Cyclic Strength

For the estimation of the cyclic strength, Tokimatsu and Yoshimi (Tokimatsu 1983) proposed a simple empirical formula which is based on N-value and the content of fine particle less than 0.074 mm. This formula is adopted in the design handbook by Architectural Institute of Japan (AIJ). Another way of estimating the cyclic strength is to use laboratory test data. While the laboratory test data using the samples from this site was not available, data from other site in Niigata city were used. (Mori 1979) The cyclic stress ratio causing initial liquefaction in 20 cycles is usually taken as the cyclic strength. The comparison described in Fig. 3 shows that the cyclic strength derived from the equation are consistent with the test data. In this study thereafter the laboratory test data are used as the cyclic strength.

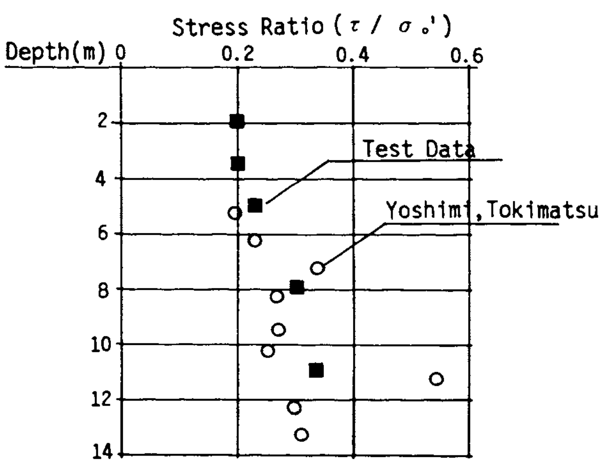

Figure 3 Comparison of Cyclic Strength

Shear Stress Level

To compute the shear stress level expected in the design earthquake, a dynamic response analysis of soil-structure model was carried out. The building was modelled by a lumped mass system and the soil was modelled by finite elements and the piles were represented by beam elements as shown in Fig. 4. The analysis was done by a total stress method and the elasto-plasticity of the soil was approximated by an equivalent linear method. The bed rock was taken at GL - 144 m, and dampers were allocated between the soil model and the bed rock. The side of the soil model was connected to a free field model through a transmitting boundary.

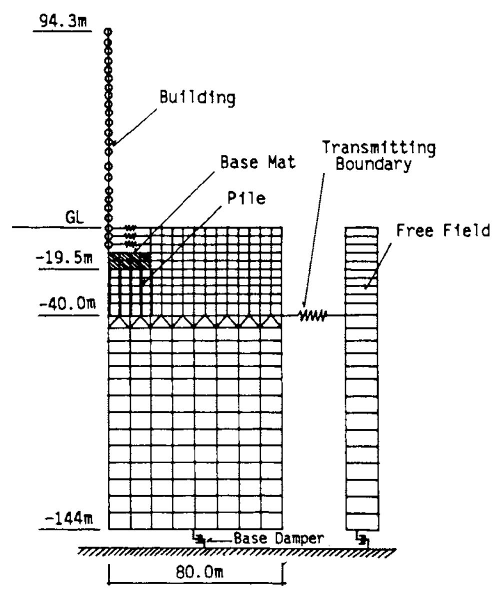

Figure 4 Soil-Structure Model for Total Stress Analysis

The record of the 1964 Niigata Earthquake at Akita City Office was selected as the input seismic motion(Ishihara 1982). Assuming the re-occurrance of the 1964 Earthquake, the predominant period of the original record of 0.675 sec was changed to 0.40 sec according to the difference of the epicentral distance (Seed 1969), by changing time increments of the wave from 0.20 sec to 0.119 sec . In the Niigata area, the maximum velocity of the design seismic wave is usually taken to be 22.5 kine at the ground surface. A one dimensional equivalent linear analysis of soil deposit model was carried out by changing the maximum acceleration of the input motion, and the input motion to the 2D model was decided so that the velocity at the ground surface was 22.5 kine.
Strain dependent property of the soil model, i.e., G-r and h-r, was modelled by linearizing the tri-axial test result of specimens taken from the site.

Figure 5 shows the distribution of the maximum acceleration in the soil between the ground surface and -40 m, along the side of the building and 40 m from the side of the building. An amplification of the acceleration between GL and GL - 15 m level is observed . The maximum acceleration of the ground surface at the foot of the building is 180 gal, which is considerably smaller than the value of 240 gal at the ground surface 40 m from the building. This is because of the effect of soil-structure interaction.

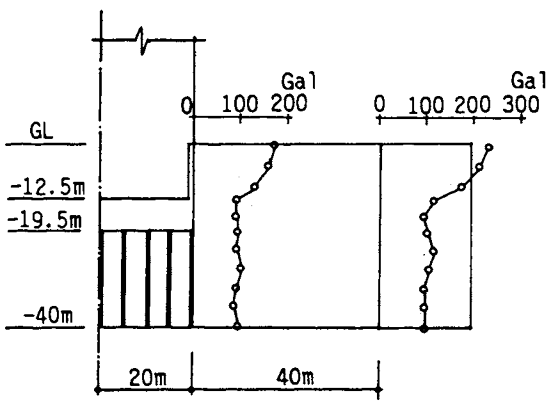

Figure 5 Distribution of Maximum Acceleration

Estimation of Liquefaction Potential

Figure 6 compares the shear stress ratio obtained from the numerical analysis, and the cyclic strength derived from the laboratory test. The shear stress ratio to be used for the comparison is 0.7 * (the maximum shear stress)/(initial effective confining stress). The reduction factor of 0.7 was selected based on the study by Ishihara (Ishihara 1976). Liquefaction is likely to occur from the ground surface to -10 m level. The stress level near the building is smaller than those at 40 m from the building, indicating that the prediction of liquefaction based on the analysis of level ground offers a conservative estimation of the liquefaction potential for the soil near the building.

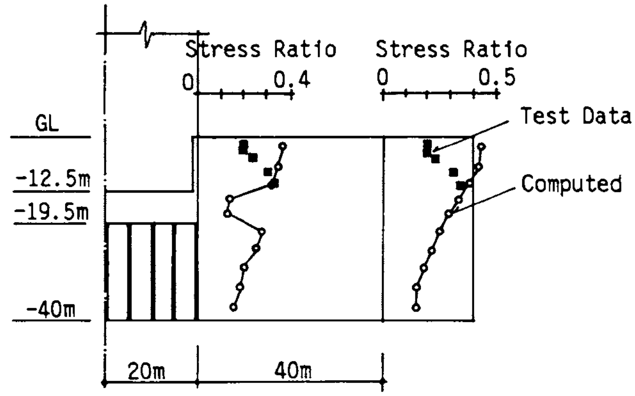

Figure 6 Comparison of Stress Ratio and Cyclic Strength

EFFECTIVE STRESS ANALYSIS

Soil Model

The constitutive model used in this analysis is the Multi Mechanism Model which was originally proposed by Hujeux and Aubry (Hujeux 1981) and modified by Kabilamany and Ishihara (Kabilamany in preparation). This model assume that the plastic shear deformations originate from three independent plane strain mechanism. Thus the total strain increment is defined from the following equations.

$$\dot{\varepsilon}_i = \dot{\varepsilon}_i^e + \dot{\varepsilon}_i^p \tag{1}$$

$$\dot{\varepsilon}_i^p = (\dot{\varepsilon}_i^p)_1 + (\dot{\varepsilon}_i^p)_2 + (\dot{\varepsilon}_i^p)_3 \tag{2}$$

where

$\dot{\varepsilon}_i$: total strain increment
$\dot{\varepsilon}_i^e$: elastic strain increment
$\dot{\varepsilon}_i^p$: plastic strain increment
$(\dot{\varepsilon}_i^p)_j$: strain increment in i th direction by j th mechanism

For each plane strain mechanism k, yield function , flow rule, and hardening rule are defined in the following way.

Yield Function

$$f_k = |q_k - c_k| - p_k h_k \sin\phi_f$$

$$c_k = \begin{cases} 0 & : \text{Loading} \\ (h_k^R - \nu_k h_k) p_k \sin\phi_f & : \text{Unloading and Reloading} \end{cases}$$

$$p_k = \frac{\sigma_i + \sigma_j}{2}$$

$$q_k = \frac{\sigma_i - \sigma_j}{2}$$

σ_i, σ_j : Principal Stress

ϕ_f : Angle of Internal Friction

h_k : Hardening Parameter

h_k^R : Hardening Parameter for Unloading

ν_k : Direction of Unloading 1 or -1

Hardening Parameter

$$h_k = \frac{\Omega_k}{a + \Omega_k}$$

$$\dot{\Omega}_k = (\dot{\varepsilon}_{vd})_k + \frac{q_k}{p_k}\left(\dot{\varepsilon}^p\right)_k$$: Increment of Normalized Plastic Work

a : Hardening Parameter Loading
Loading a^m Unloading and Reloading a^c

Flow Rule

$$\frac{(\dot{\varepsilon}^p_{vd})_k}{\left(\dot{\varepsilon}^p\right)_k} = \mu_k - \left|\frac{q_k - c_k}{p_k}\right|$$

$$(\dot{\varepsilon}^p_{vd})_k = (\dot{\varepsilon}^p_i)_k + (\dot{\varepsilon}^p_j)_k$$

$$\left(\dot{\varepsilon}^p\right)_k = (\dot{\varepsilon}^p_i)_k - (\dot{\varepsilon}^p_j)_k$$

$$\mu_k = \frac{3\mu}{\mu + 6}$$: Dilatancy Parameter

$$\mu = c + \frac{2}{\pi}(\mu_f - c)\,\mathrm{Tan}^{-1}\left(\frac{\varepsilon^p}{s_c}\right)$$: Stress Ratio at Phase Transformation

Table 1 lists the soil constants used for the computation. The density of skelton and porosity n, were determined from the laboratory test of soil specimens taken from the site and the coefficient of permeability was roughly estimated from the field test. The shear modulus G was computed from the shear wave velocity measured at the site. M is a function of a failure angle which was assumed from N-value. As the dilatancy parameters C, S, and μ , the values which Kabilamany obtained for Fuji river sand were used (Kabilamany 1986).

The hardening parameters a^m a^c can not be decided theoretically nor experimentally. Simulation of a triaxial test using single element numerical model by varying these hardening parameters were carried out, and the values of a^m a^c with which a curve of the cyclic stress versus the number of cycles until liquefaction (liquefaction strength curve) was best fit, were determined and used in the analysis. As the liquefaction strength curve of the soil from the site was not available, the curves for the Sewage Treatment Site in Niigata City obtained by Ishihara was used for the curve fitting. Figure 7 shows the result of the element test simulation.

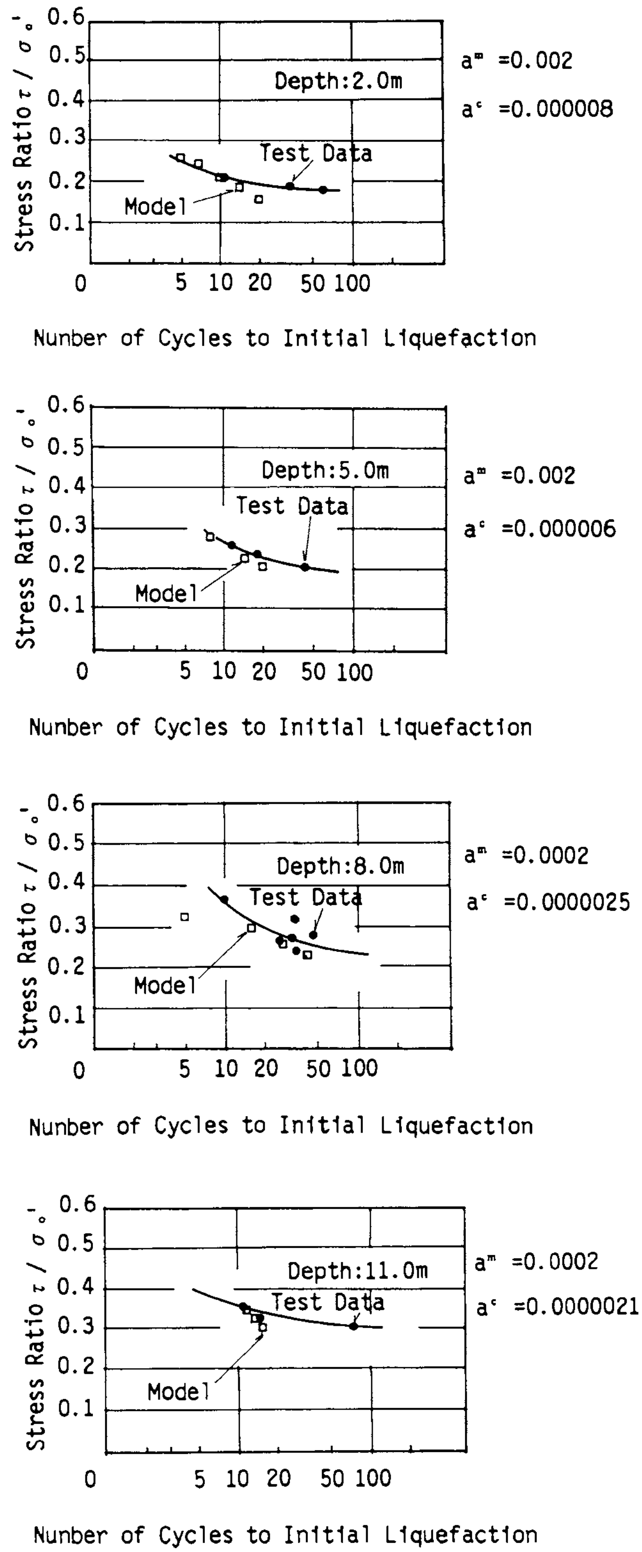

Figure 7 Element Test Simulation

Table 1 Parameters for Soil Model

		GL ~ -14m	-14m ~ -40m
Young's Modulus	E(KN/m²)	1.48E5	2.21E5
Poisson's Ratio	ν	0.200	
Shear Modulus	G(KN/m²)	6.17E4	9.21E4
Bulk Modulus (Particle)	(KN/m²)	5.00E7	
Bulk Modulus (Fluid)	(KN/m²)	2.00E6	
Density(Skelton)		2.63	
Density(Fluid)		1.00	
Porosity	n	0.448	
Permeability	(m/s)	1.00E-4	
M		*1.20/1.42/1.50/1.55	1.64
C		0.45	
S		0.0035	
μ		1.113	

* values for 1st~4th layer

Numerical Model

Figure 8 shows the numerical model. The building was modelled by a frame model and the pile was modelled by a beam element. The soil deposit was modelled to the depth of - 40 m and the bottom of the soil model had a fixed condition. At both sides of the soil model, the horizontal displacement of each end node at the same level were tied, i.e. having equal displacement, and the vertical displacement was restricted to be zero. For comparison one dimensional soil deposit model described in Fig. 8 was also compute.

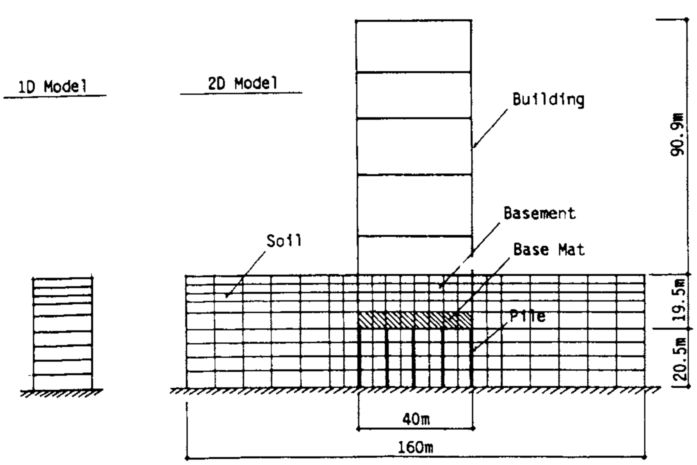

Figure 8 Numerical Model for Effective Stress Analysis

Numerical Result

1) 1 D model------ The compute acceleration time histories at several depth are shown in Fig. 9 where it is noted that liquefaction in the second layer (-3 m to -6 m) occurred around 5 sec after the initiation of the shaking and the amplitude of acceleration at the surface did not increase after this point. Because of the liquefaction, the decrease of the maximum acceleration is observed near the surface as plotted in Fig. 10.

Figure 11 shows the time history of excess pore water pressure, effective stress path, and shear stress-strain curve of the second layer, where liquefaction and resulting stiffness degradation are clearly seen. The occurrence of liquefaction near the surface is in accord with the prediction of liquefaction potential from the total stress analysis described previously.

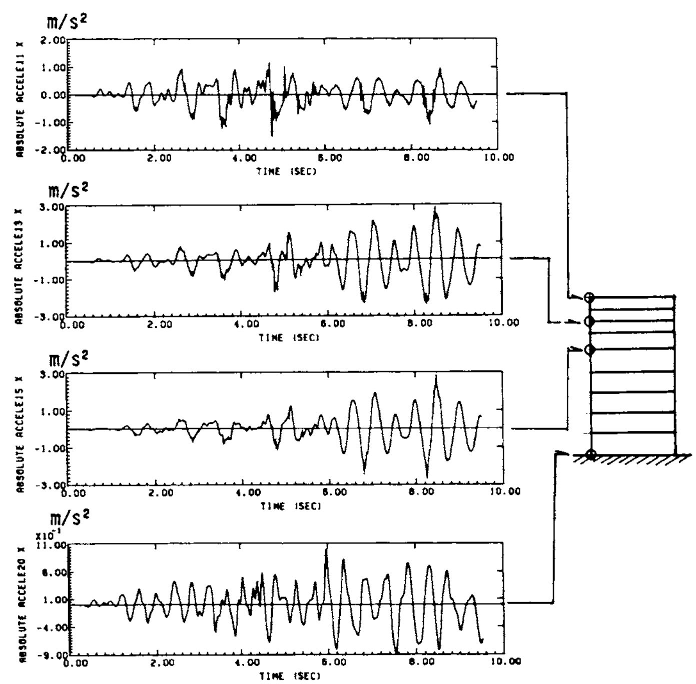

Figure 9 Acceleration Time History

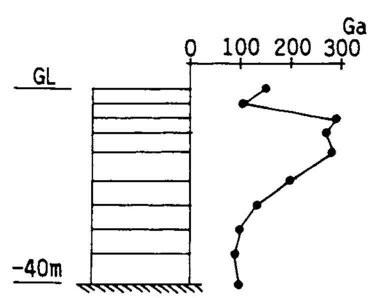

Figure 10 Distribution of Maximum Acceleration

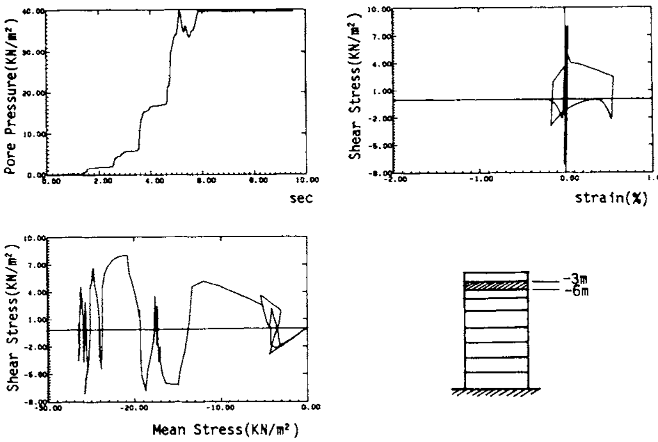

Figure 11 Response of Liquified Layer

2) 2D Model--- Figure 12 shows the elements where liquefaction occurred (elements where mean stress became zero). Liquefaction occurred in five elements in the first layer and one element in the second layer, which is approximately in accord with the result of 1D model analysis and with the prediction of liquefaction by the total stress analysis.

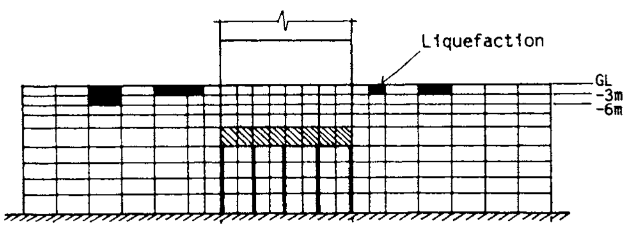

Figure 12 Elements where Liquefaction Occurred

The computed acceleration time history at several locations are shown in Fig. 13, and the distribution of the maximum acceleration at locations adjacent to the basement of the building and the location 40 m from the side of the building are plotted in Fig. 14.

The acceleration near the building is smaller than the values at 40 m away from the building, which is in accord with the result of the total stress analysis as described in Fig. 5. The amplification of the acceleration near the surface, which is observed in the total stress analysis, however, is not observed in the effective stress analysis. This difference of the result may be attributed to the difference of the numerical methods of 1) equivalent linear modelling vs elasto-plastic modelling, and 2) total stress method vs effective stress method, though it is not clear which difference have larger effect. The effective stress analysis offered a smaller maximum acceleration than total stress analysis.

In comparison with the 1D effective stress analysis, clear effect of liquefaction on the acceleration, i.e. decrease above the liquefied layer is not observed in the 2D analysis. This is caused by the fact that the movement of the ground near the building is smaller than free field and as a result not all elements in a layer reach liquefaction at the same time in the 2D analysis. This result suggests that 1D analysis may offer a conservative estimation of liquefaction potential for the soil-structure system.

Figure 15 shows the time history of excess pore water pressure , effective stress path, and shear stress-strain curve at several elements. At the elements adjacent to the building, the pore water pressure changes according to the change of the shear stress ,but did not build up , while pore water pressure build-up is observed at locations 40 m away from the building. Near the building, large plastic deformation of the soil is observed , which resulted in the small amplitude of acceleration near the ground surface.

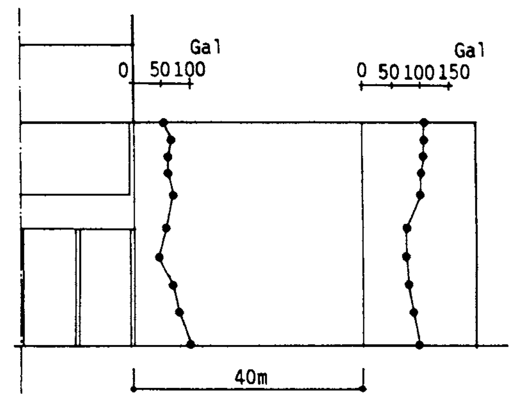

Figure 14 Distribution of Maximum Acceleration

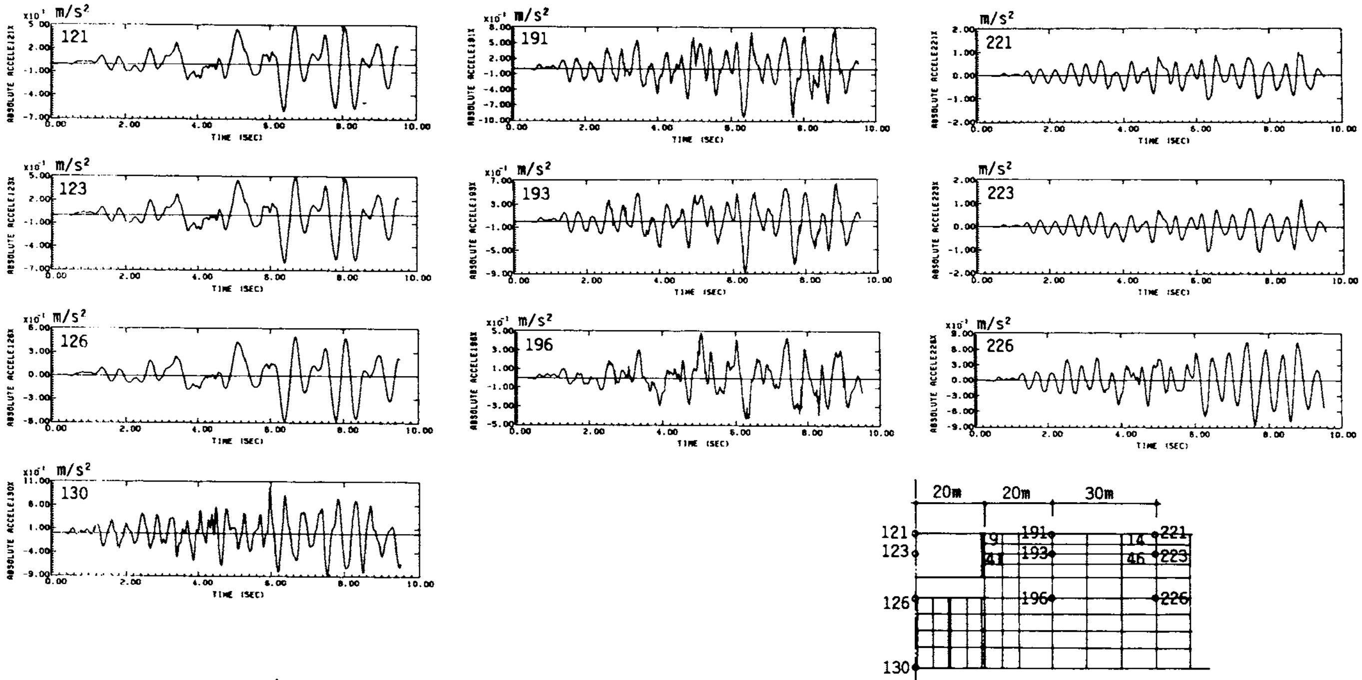

Figure 13 Acceleration Time History

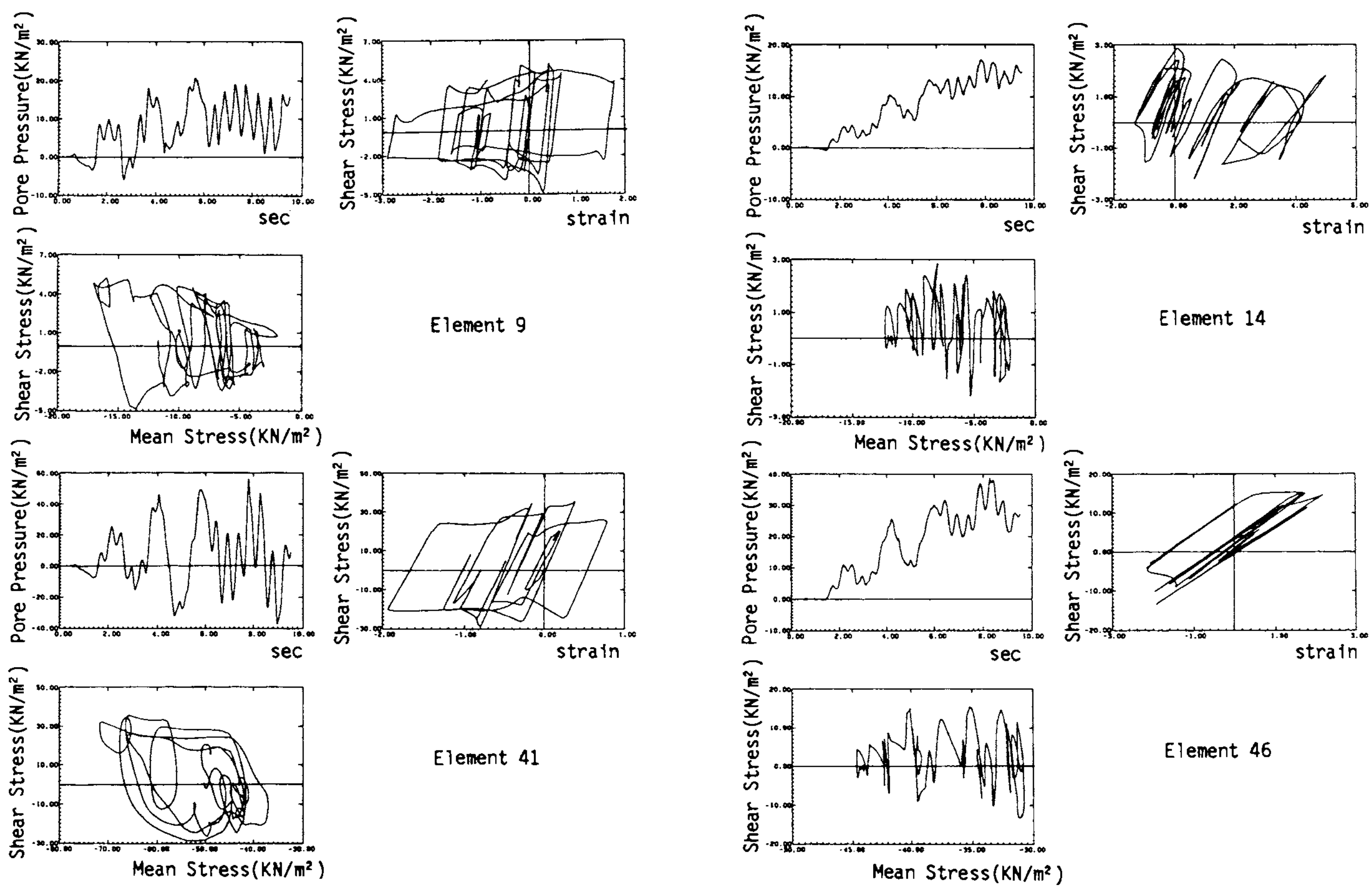

Figure 15 Response of Elements

CONCLUSIONS

For the prediction of the liquefaction potential of a high rise building, a total stress analysis of a soil-structure model was carried out. An effective stress analysis of 1D and 2D model was also conducted. From the comparison of these analyses, the liquefaction observed in the effective stress analysis shows approximately in accord with the expectation from the total stress analysis. The liquefaction effect in 1D model analysis was clearer than in 2D model analysis. The difference of the soil behavior and the pore water build-up characteristics near the structure and away from the structure was observed in the 2D model analysis .

REFERENCES

Tokimatsu, K. and Yoshimi, Y. (1983), " Empirical Correlation of Soil Liquefaction Based on SPT N-Value and Fines Content", Journal of Institute of Soil Engineering, Vol. 23, No. 4 : 56 - 74.

Mori, K. and Ishihara, K. (1979), " Undisturbed Block Sampling of Niigata Sand", Proc. 6th Asian Regional Conf. Soil Mechanism and Foundation Engineering, Singapore : 39 - 42.

Ishihara, K. and Towhata, I. (1982), " Dynamic Response Analysis of Level Ground based on the Effective Stress Method ", Soil Mechanics, John Wiley & Sons Ltd.

Seed, H. B., Idriss, I. M. and Kiefer, F. W. (1969), " Characteristics of Rock Motions During Earthquakes ", ASCE, SM 5 : 1199 - 1218.

Ishihara, K. (1976), Fundamentals of Soil Dynamics, Kajima Publishing, Tokyo (in Japanese).

Hujeux, J. C. and Aubury, D. (1981), " A Critical State Type Stress-strain Law for Monotonous and Cyclic Loading ", Proc. of the Symposium on Implementation and Stress-Strain Laws in Geotechnical Engineering, Chicago : 657 - 671.

Kabilamany, K. and Ishihara, K. (in preparation), " Stress Dilatancy Relationship and Yield Surface for Sand in the Context of Multiple Mechanism", submitted to the Soil and Foundation.

Kabilamany, K. (1986), " Modelling of Cyclic Behavior of Sand and its Application to Seismic Response Analysis ", Doctoral Thesis, The University of Tokyo.